

X-ray biomedical imaging beamline at SSRF

To cite this article: H Xie *et al* 2013 *JINST* **8** C08003

View the [article online](#) for updates and enhancements.

You may also like

- [Application of real-time digitization techniques in beam measurement for accelerators](#)
Lei Zhao, , Lin-Song Zhan et al.
- [Study of closed orbit response to magnet vibrations at the SSRF storage ring](#)
Chen Jian-Hui, Zhao Zhen-Tang, Dai Zhi-Min et al.
- [Beam dynamics of the superconducting wiggler on the SSRF storage ring](#)
Qing-Lei Zhang, , Shun-Qiang Tian et al.



ECS
The
Electrochemical
Society
Advancing solid state &
electrochemical science & technology

DISCOVER
how sustainability
intersects with
electrochemistry & solid
state science research

7th MEDICAL APPLICATIONS OF SYNCHROTRON RADIATION WORKSHOP (MASR 2012)
SHANGHAI SYNCHROTRON RADIATION FACILITY (SSRF),
17–20 OCTOBER, 2012

X-ray biomedical imaging beamline at SSRF

H. Xie, B. Deng, G. Du, Y. Fu, Y. He, H. Guo, G. Peng, Y. Xue, G. Zhou, Y. Ren,
Y. Wang, R. Chen, Y. Tong and T. Xiao¹

*Shanghai Synchrotron Radiation Facility(SSRF), Shanghai Institute of Applied Physics,
Chinese Academy of Sciences(CAS),
Zhangheng Road 239, 201204 Shanghai, China*

E-mail: txxiao@sinap.ac.cn

ABSTRACT: Since May 6, 2009, the X-ray biomedical imaging beamline at Shanghai Synchrotron Radiation Facility (SSRF) has been formally opened to users. The beamline is composed of a wiggler source with the intensity of magnetic field of 2.0 Tesla, a double crystal monochromator (DCM) cooled with liquid nitrogen, a 6-axis filter for high heat load reducing on the downstream optics such as Be window and DCM. The photon energy range for the monochromatic beam is 8–72.5keV. Three sets of digital X-ray detectors are provided to users with the pixel size range being 0.37–13 μ m. Several imaging methods such as micro-CT, in-line phase contrast imaging could be applied in biomedicine, material science and paleontology studies. The spatial resolution of 0.8 μ m and the temporal resolution of 1 ms could be realized. By the end of 2012, the beamline has provided more than 13900 hours beamtime for users, while over half of the research proposals come from biomedicine field. Nearly 2000 person-times have come and done their experiments at the beamline. More than 470 user proposals have been performed and more than 110 papers from users have been published. Some typical experimental results on biomedical applications will be introduced.

KEYWORDS: Computerized Tomography (CT) and Computed Radiography (CR); Medical-image reconstruction methods and algorithms, computer-aided so

¹Corresponding author.

Contents

1	Introduction	1
2	Beamline and endstation	2
2.1	Beamline	2
2.2	End-station	2
3	Methodology development	4
3.1	Quantitative phase-contrast micro-CT	4
3.2	Spiral micro-CT	7
3.3	Fluorescence CT	8
4	User operation	8
5	Summary	9

1 Introduction

The X-ray imaging and biomedical applications beamline at SSRF devotes itself to developing methodology and application study of dynamic in-line X-ray phase-contrast imaging (IL-PCI), X-ray microscopic computed tomography (Micro-CT) and other novel X-ray imaging techniques. The beamline aims at two major scientific goals. The first goal is to realize low dose, non-destructive, high resolution, dynamic and 3-dimensional X-ray imaging for the inner microstructures of soft tissues and low Z materials. And the second goal is to realize non-destructive, high resolution, 3-dimensional X-ray imaging for the inner microstructures of paleontology, archaeology and geology samples. The designed goals and the test results of this beamline have been shown in table 1, which indicate that these goals have been achieved.

Tomography reconstruction for a set of 1000 projections can be completed within 5 minutes and a remote micro-CT reconstruction system has been developed and opened to users. Some research results of phase retrieval algorithm of in-line phase contrast imaging have been published on Optics Letters [1] and Optics Express [2]. X-ray fluorescence CT and spiral micro-CT methods also have been built. Other X-ray imaging methods such as local micro-CT, coherent X-ray diffraction imaging and X-ray phase-contrast imaging with grating interferometer are also being developed.

Many experiments for different kinds of samples, such as biological soft tissues, paleontologic fossils, alloy materials and so on, have been carried out at this beamline and some good imaging results have been obtained. Based on these experimental results, nearly 50 papers included in SCI have been published, such as 1 paper on “Current Biology” [3], 1 paper on “Biomaterials” [4], 1 paper on “Molecular and Cellular Biology” [5], 2 papers on “Stoke” [6]–[7]. Some typical experimental results on biomedical applications will be introduced.

Table 1. Acceptance test results of designed goals.

		Designed goals	Test results
Beam model		Unfocused monochromatic beam	Unfocused monochromatic beam
Imaging method		PCI and μ -CT	PCI and μ -CT
Energy range		10–60keV	8–72.5keV
Energy resolution($\Delta E/E$)		$< 5 \times 10^{-3}$	$< 3 \times 10^{-3}$
Maximal beam size		45mm(H) \times 5mm(V) @30m@20keV	48mm(H) \times 5.30mm(V) @34m@20keV
Photon flux density		1×10^9 phs/s/mm ² @20keV@200mA	1.9×10^{10} phs/s/mm ² @20keV@200mA
Spatial resolution	Dynamic PCI	$\leq 20\mu\text{m}$ @5frame/s	$15\mu\text{m}$ @6.5frame/s
	Static PCI	$\leq 5\mu\text{m}$	$3.0\mu\text{m}$
	Absorption contrast imaging	$\leq 3\mu\text{m}$	$1.5\mu\text{m}$
	Phase-contrast CT Imaging	$\leq 20\mu\text{m}$	$9.5\mu\text{m}$
	Absorption-contrast CT Imaging	$\leq 10\mu\text{m}$	$9.5\mu\text{m}$

2 Beamline and endstation

2.1 Beamline

The light source of the beamline is an 8-period hybrid-type wiggler source. The periodic length is 14cm. The maximum K-value is 24.8 at minimum wiggler magnet gap of 17 mm. The fundamental radiation covers the energy range of 8.0–72.5keV by tuning the magnet gap from 17 to 35 mm. The heat load power of 10kW is a big challenge for this beamline and is controlled in an acceptable range by tuning the gap for different optimized energy range.

The sketch layout of the beamline is shown in figure 1. A white beam slit is placed at 20m away from the source point. The maximum aperture size of the slit is 30mm \times 4mm. A graphite filter is placed behind the white beam slit to absorb low-energy photons and reduces the heatload on downstream water-cooling beryllium window and the monochromator. The filter consists of six water-cooled filter banks and each filter bank consists of two beam apertures and two highly-oriented pyrolytic graphite foils. Several filter foils of different thickness can be combined into the beam for different wiggler gap. The monochromator is a constant-exit double crystal cryogenic-cooling monochromator placed at 28 m away from the source point. Two sets of Si (111) and Si (311) orientation crystals can be on-line exchanged.

2.2 End-station

The BL13W1 end-station can offer several non-destructive high-resolution 3-dimensional X-ray imaging techniques. Figure 2 is the photo of the end-station. A long slide rail (8m) on the two experimental tables is used to adjust the imaging distances between samples and detectors for

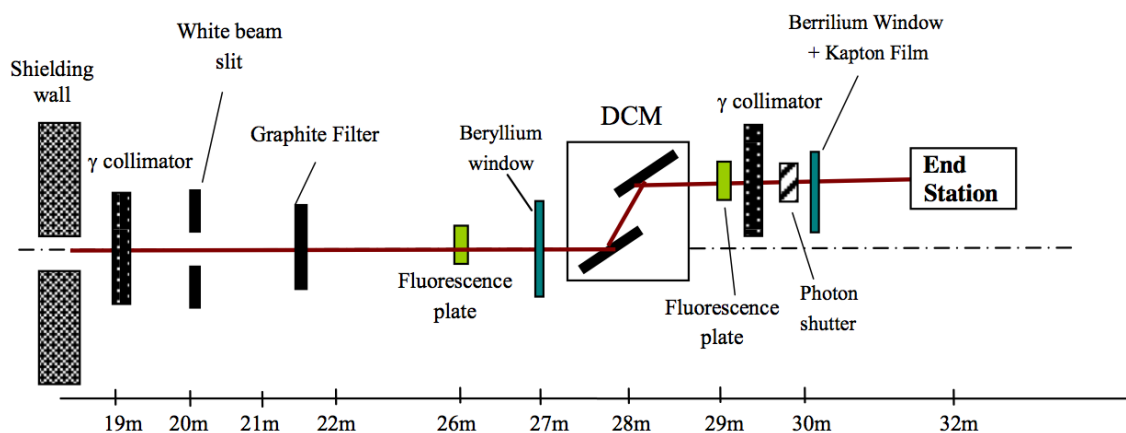


Figure 1. Sketch layout of the beamline.



Figure 2. Photo of the end-station.

in-line phase contrast imaging. A sample stage can translate and rotate in three axes direction with resolution better than 1 micron. An ionization chamber is used to monitor the incident x-ray intensity. The BL13W end-station has four different kinds of X-ray detectors with different spatial resolution. The pixel size range is from $0.19\mu\text{m}$ to $24\mu\text{m}$. An X-ray fluorescence detector is provided for X-ray fluorescence micro-CT (XFCT) method.

Synchrotron-based X-ray micro-computed tomography (SR μ -CT) is nowadays a powerful non-destructive, high-resolution imaging technique. A fast micro-CT reconstruction system has been established at BL13W1, which is very convenient for users. The processing time of micro-CT reconstruction has been decreased to 5 minutes and a remote data processing and transfer system has been realized and opened to users. The fast CT reconstruction system includes two parts: GPU parallel computing server and micro-CT reconstruction software. The GPU parallel computing server consists of a WEB server, a file server, a head node and a computational node, using Win-

dows HPC Server 2008 cluster environment. The GPU core with the parallel processing ability greatly improves the processing speed and realizes the acceleration of 112 times. A fast micro-CT reconstruction software called as X-TRACT SSRF has been developed under the international cooperation with the CSIRO in Australia and opened to users. The number of registered users is about 100. The users can visit the website <https://ct.ssrif.ac.cn> to download the client software X-TRACT SSRF.

The ring artifacts in micro-CT reconstructed images, which are mainly introduced by non-uniform responses of the detector pixel elements, greatly influence 3D reconstruction qualities and quantitative analyses. A correction algorithm based on the polar coordinate transformation has been developed [8]. Firstly, through the polar coordinate transformation, ring artifacts are transformed to line artifacts. Then, a Fourier transform is applied to the line artifacts image and a frequency domain filtering process is performed with a 2D low pass filter. Finally, a corrected image is got by the inverse transform process both Fourier and coordinates. The corrected image results indicate that the proposed algorithm not only eliminates the ring artifacts effectively, but also keeps the image edges and increase the SNR.

3 Methodology development

Several X-ray imaging methods have been developed at the X-ray imaging and biomedical applications beamline. Some research achievements on phase retrieval methods of in-line phase contrast imaging [1-2, 9], X-ray fluorescence CT [10]–[11] and spiral micro-CT [12] method have been published. Other X-ray methods such as local micro-CT, coherent X-ray diffraction imaging and X-ray phase-contrast imaging with grating interferometer also are being developed.

3.1 Quantitative phase-contrast micro-CT

Our group of SSRF X-ray imaging beamline has developed three kinds of methods of quantitative in-line phase-contrast micro-CT, which are phase retrieval with a single distance PPCT data, phase retrieval with two distances PPCT data and phase retrieval based on phase-attenuation duality (PAD) respectively.

The Modified Bronnikov algorithm (MBA) [13], which is revised based on Bronnikov algorithm [14], is a method to direct reconstruct three-dimensional (3D) refractive index from single sample to detector distance (SDD) X-ray propagation-based phase-contrast tomography (PPCT) data [14]. However, the absorption correction factor (ACF) value in MBA was determined using a semi-empirical approach, which may be cumbersome and time-consuming since the ACF is varying with samples, and thus inconvenient in general applications. We proposed an approach to determine ACF values simply and accurately for MBA algorithm [1]. This approach is based on phase-attenuation duality that is valid for quasi-homogeneous and weakly absorbing samples [15]. It takes into account the wavelength, SDD and phase-attenuation duality of PPCT. Moreover, a practical method for calculating the optimal phase-attenuation duality value directly is proposed based on the first Born-type approximation phase-retrieval algorithm [16]. The method has been evaluated with experimental PPCT data collected at BL13W1. A set of micro-tomography data of a sample with wires of nylon, polystyrene and PMMA was obtained at 18keV. The effective pixel size of the X-ray CCD is $3.7\mu\text{m}$ and the SDD is 20cm. The reconstructed result was shown in

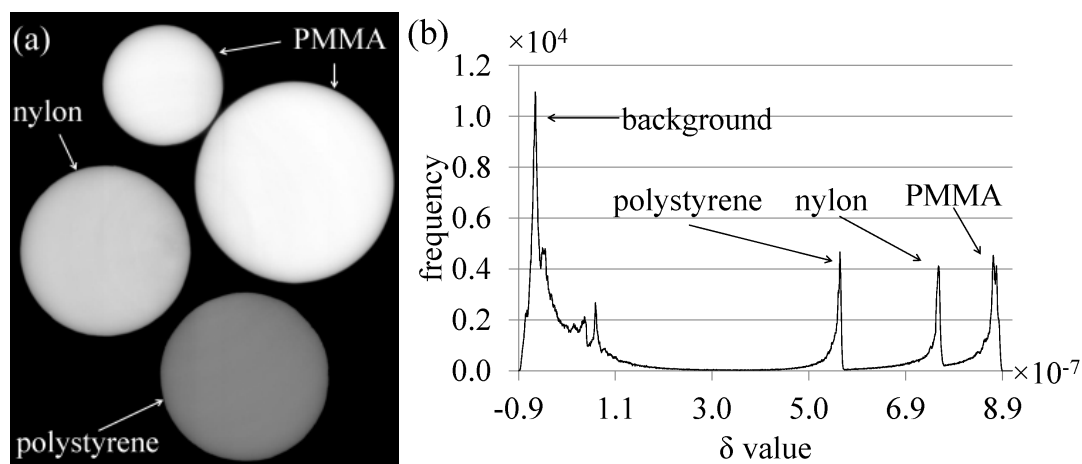


Figure 3. Experimental results: (a) Reconstructed result of the wire sample. (b) Histogram of figure 3a, the labels indicate the peak for each material.

figure 3a and figure 3b shows the histogram of figure 3a. As the both images show, these three kinds of materials can be well distinguished with the proposed phase retrieval method and there is a qualitative agreement with ideal values, which are polystyrene ($7.24e-7$) < nylon ($8.01e-07$) < PMMA ($8.23e-07$).

Since the simplicity of recording and the flexibility of post-processing, phase retrieval from single sample-to-detector distance (SDD) image has found applications in many fields up to now. However, it has suffered from disadvantages when it was used in the case of complicated samples or with high precision required, for instance, the quantitative retrieval of biological tissues. On contrary, phase retrieval with multiple SDD images could improve the precision apparently in quantitative X-ray in-line phase contrast imaging. Among all the related phase retrieval approaches, the two-SDDs-image-based one is the simplest and well compromises between precision and dose. However, as depicted in ref. [2], the critical point that determines the retrieval efficiency of this method is the optimization of SDD z_1 and z_2 . Y. Ren, et al. [2] investigated the problem systematically based on computer simulation and related experiments using phase retrieval algorithm based on the first-order Born approximation. They introduced the root-mean-square (RMS) criterion [16]–[17] to evaluate the relative errors of retrieved images to real one and the spectral correlation degree (SCD) to evaluate the pertinence between the two SDD images. Experiments were performed at the X-ray imaging beamline BL13W at Shanghai Synchrotron Radiation Facility (SSRF). The results show that the highest retrieving precision could be obtained with $z_2=3z_1$, as shown in figure 4, which gives the RMS curves vs. z_2 in spite of different z_1 values. The investigation shows that the retrieving precision of less than 8% could be achieved with the optimized method and it could find practical applications in many fields, such as biomedicine, material science, geology, paleontology etc., where relatively higher precision quantitative information is required. Combined with micro-CT, higher density resolution should be achievable.

X-ray tomography of samples containing both weakly and strongly absorbing materials are necessary in material and biomedical imaging. Extending the validity of the phase-attenuation duality (PAD) method [15], the propagation-based phase-contrast computed tomography (PPCT)

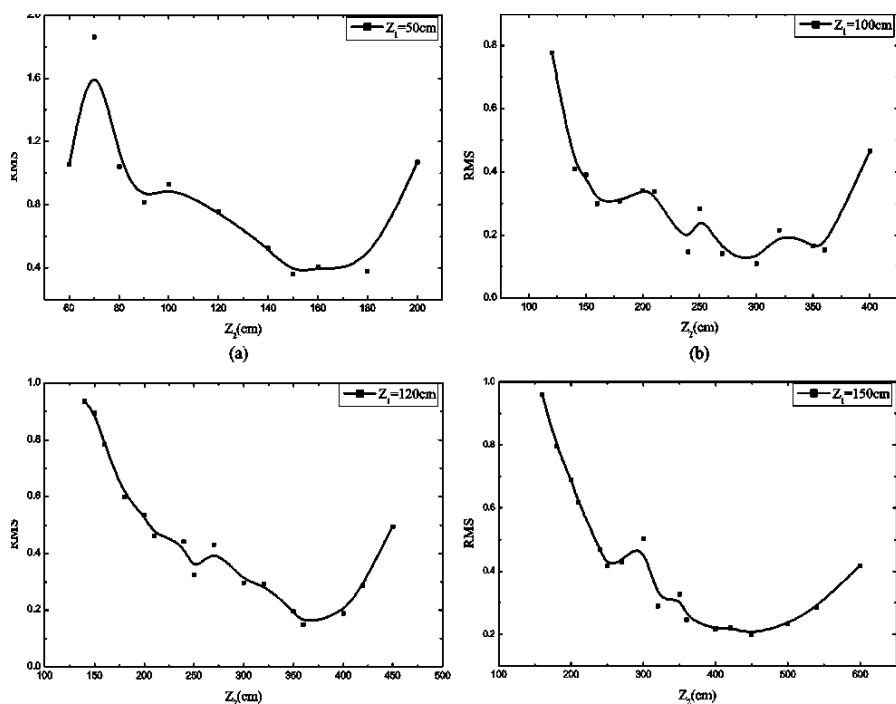


Figure 4. Retrieving errors vs. z_2 , while z_1 was set to (a) 50cm, (b) 100cm, (c) 120cm and (d) 150cm, respectively.

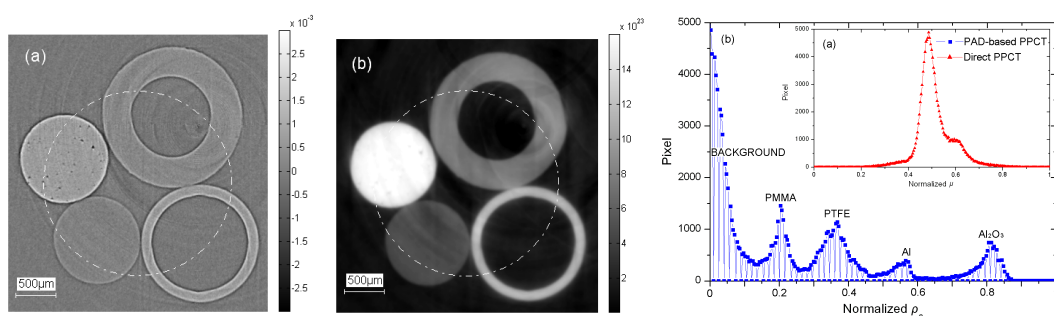


Figure 5. Reconstructions and histograms of the electron density distribution of the samples with (a) direct and (b) PAD-based PPCTs at 60keV.

of a sample with hybrid compositions of both the light and dense components with energy of 60 keV of synchrotron radiation is investigated. The experimental results show that the PAD-based PPCT is effective in imaging both the weakly and strongly absorbing components simultaneously. Compared with the direct PPCT technique, the PAD-based PPCT technique demonstrates its excellent capability in material discrimination and characterization (See figure 5). In addition, the PAD-based PPCT exhibits a striking performance on the image contrast enhancement and noise suppression. Therefore, this technique is useful for material and biomedical imaging applications, especially when the radiation dose involved imposes a serious constraint. The results has been published at *Chinese Optics Letters*, 10(12), 121101(2012) [9].

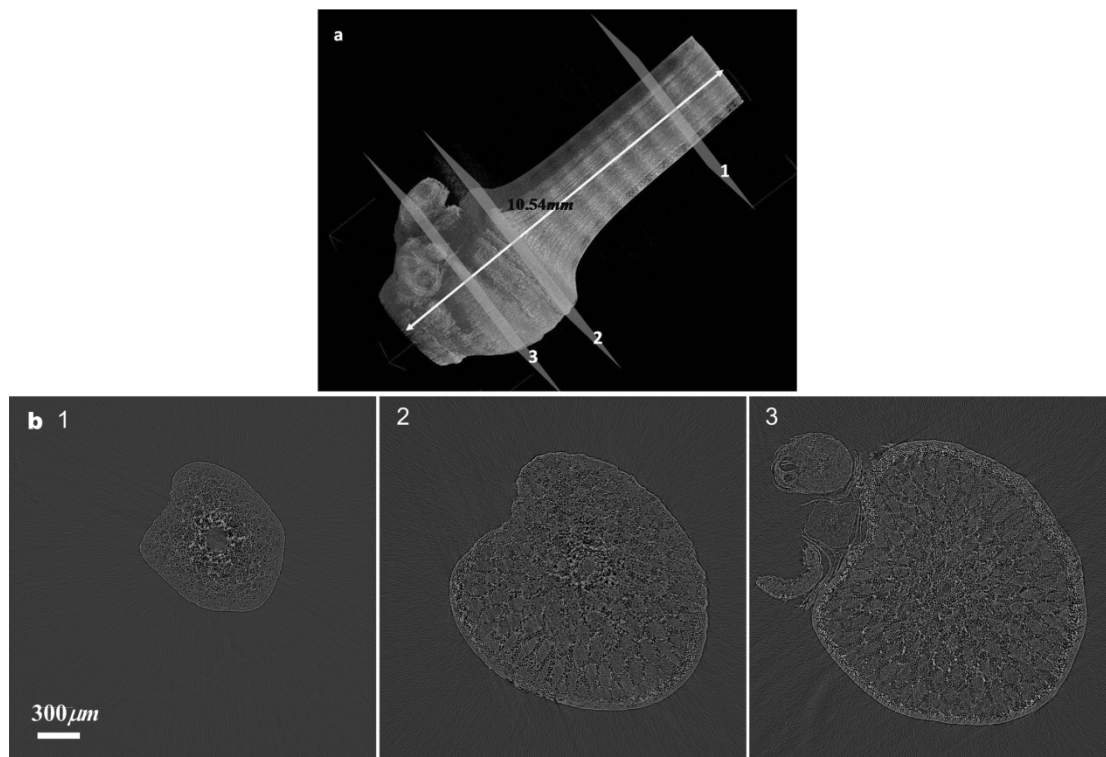


Figure 6. SRS μ -CT reconstructed images of bamboo. (a) 3D image. (b) Reconstructed slices. '1, 2, 3' referred to planes marked '1, 2, 3' in (a) respectively.

3.2 Spiral micro-CT

Synchrotron X-ray beam is prolate and the horizontal size is much bigger than vertical one, e.g. the maximum beam size of BL13W at SSRF is $50\text{mm} \times 5\text{mm}$. For the samples which are longer than the X-ray beam vertical size, it is difficult to obtain three dimensional (3D) images with high spatial resolution in a single scan. These samples are usually scanned section by section and the 3D images are spliced of all these pieces, this is a complicated, slow processing. Spiral scanning has been introduced into SR μ -CT to resolve the problem. SR-based spiral μ -CT (SRS μ -CT) is able to obtain volumetric projection data of a long sample in one continuous scan, which has the advantages of short acquisition time, high spatial resolution and less artifacts.

SRS μ -CT experimental system has been built at BL13W at SSRF [12]. The sample stage is composed of a rotating platform and a lifting stage. The sample is scanned in spiral mode by synchronized movement of two stages. The reconstructed program has been completed which is based on filtered back projection (FBP) algorithm with a pre-processing of rearrangement of sonogram [18]. The effect of some factors on image quality and scanning speed have been investigated such as pitch, vertical beam width and projections per 180° , and the experimental parameters have been optimized on the basis of the investigation. SRS μ -CT experiment of bamboo was performed at SSRF. The 3D image and slices were obtained with high spatial resolution, as shown in figure 6. It is found that the length of scanned bamboo was 10.54mm which was 2.73 times of vertical beam size and inner structures such as fibres were clearly displayed.

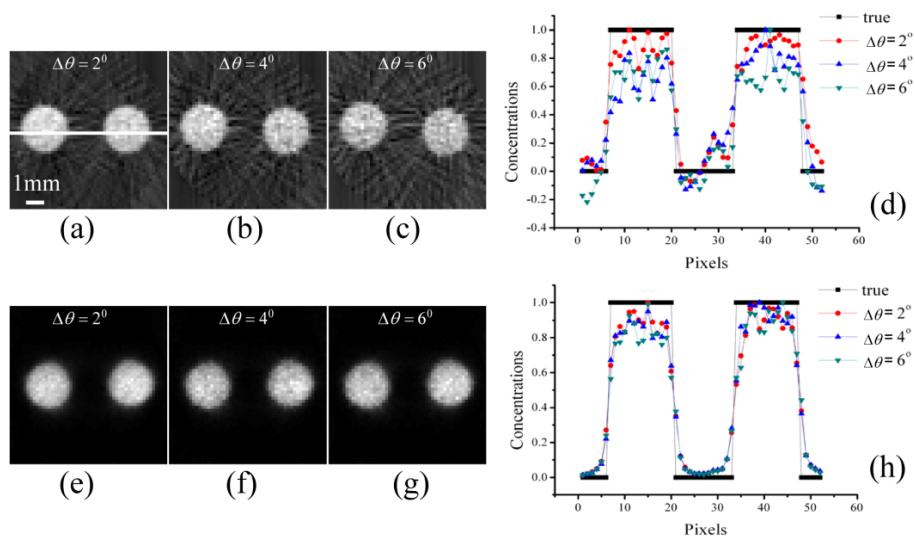


Figure 7. Cd distribution in test sample with different algorithm Upper:FBP; Down: OSEM.

3.3 Fluorescence CT

X-ray fluorescence computed tomography (XFCT) is a stimulate emission tomography that allows non-destructive reconstruction of elements distribution in the sample and has been applied in many fields. The XFCT system was established at Shanghai Synchrotron Radiation Facility (SSRF) and experimental results were obtained at the X-ray imaging (BL13W1) and hard X-ray micro-focusing beamline (BL15U1) [10]–[11]. Internal element imaging of the hair and the Fe and Zn distributions in the rat liver were reconstructed by XFCT at SSRF. Recently, ordered-subsets expectation maximization (OSEM) algorithm has been introduced into XFCT to speed up the data acquisition process. We are now studying accelerating X-ray fluorescence CT based fast scanning and OSEM (see figure 7). The results have been published at *Journal of Synchrotron Radiation* 2012, 19: 210–215 [10]

4 User operation

By the end of 2012, beamtime of more than 13900 hours were provided for users, while the distribution ratio in research fields among biomedicine, material science, environmental science and archaeology is 7.3:4.7:1.4:1. Nearly 2000 person-times have come and done their experiment on the beamline. More than 470 user proposals have been performed and more than 110 user’s papers have been published.

Synchrotron radiation angiography may provide a novel solution to directly monitor the success of middle cerebral artery occlusion. Prof. Yang group randomly prepared twenty adult Sprague-Dawley rats for middle cerebral artery occlusion models with different suture head silicone coating, and then performed the in vivo imaging at beam line BL13W1, SSRF. Silicone-coated suture was superior to uncoated suture for producing consistent brain infarction. Additionally, silicone coating length was an important variable controlling the extent of the ischemic lesion: infarcts affected predominantly the caudate-putamen with large variability (<2 mm), both the cortex and

caudate-putamen (2–3.3 mm), and most of the hemisphere, including the hypothalamus (>3.3 mm) (Stroke 43 (2012) 888–891) [7].

TIEG1 can induce apoptosis of cancer cells, but its role in inhibiting invasion and metastasis has not been reported and is unclear. Prof. Wu group found that the decreasing TIEG1 expression is associated with the increasing EGFR expression in breast cancer tissues and cell lines. TIEG1 significantly inhibits breast cancer cell invasion, suppresses mammary tumorigenesis in xenografts in mice, and decreases lung metastasis by inhibition of EGFR gene transcription and the EGFR signaling pathway. The microangiography for blood vessels was performed at beamline BL13W1 of SSRF and the results showed that TIEG1 binds the EGFR promoter to inhibit its transcription inducing the reduction of VEGF and reducing the neovascularization (Molecular and Cellular Biology 32 (2012) 50–63) [5].

With the application of Scanning Electron Microscope (SEM) and SR- μ CT of SSRF, the research group headed by Prof. Xi-guang Zhang successfully examined the crustacean fossils mainly focusing on a few phosphatocopines with nearly complete preservation of stalked eyes, antennula and limbs. The result was reported in Current Biology (22 (2012) 2149–2154) [3]. SEM has been well applied for examining details of the microstructure in the outer surface of these fossils during the investigation, and SR- μ CT at BL13W1 provided precise data concerning the internal structures that are unable to be determined by SEM technology alone.

5 Summary

After three years' user operation, the user community of the BL13W1 beamline has been built, half of them being biomedicine users and its biomedical applications have gotten remarkable achievements. Micro-CT and dynamic imaging are dominating methods at the beamline. Driven by user requirements, quantitative CT imaging techniques is being developed, especially for phase retrieval in propagation based phase contrast imaging. Other X-ray methods such as local micro-CT, coherent X-ray diffraction imaging and grating based phase-contrast imaging are being developed.

Acknowledgments

This work was supported by National Basic Research Program of China grant 2010CB834301, CAS-CSIRO cooperation research project grant GJHZ1303, the National Natural Science Foundation of China grant U1232205/A0802, 11105213, 31100680 and 51274054.

References

- [1] R.C. Chen et al., *Phase retrieval in quantitative x-ray microtomography with a single sample-to-detector distance*, *Opt. Lett.* **36** (2011) 1719.
- [2] Y.Q. Ren et al., *Optimization of image recording distances for quantitative X-ray in-line phase contrast imaging*, *Opt. Express* **19** (2011) 4170.
- [3] X.G. Zhang et al., *The First Stalk-Eyed Phosphatocopine Crustacean from the Lower Cambrian of China*, *Current Biol.* **22** (2012) 2194.

- [4] C.L. Dai. et al., *Osteogenic evaluation of calcium/magnesium-doped mesoporous silica scaffold with incorporation of rhBMP-2 by synchrotron radiation-based μ CT*, *Biomaterials* **32** (2011) 8506.
- [5] W. Jin et al., *TIEG1 inhibits breast cancer invasion and metastasis by inhibition of 2 EGFR transcription and the EGFR signaling pathway*, *Molec. Cell. Biol.* **32** (2012) 50.
- [6] F.L. Yuan et al., *Netrin-1 hyperexpression in mouse brain promotes angiogenesis and long-term neurological recovery after transient focal ischemia*, *Stroke* **43** (2012) 838.
- [7] Y.J. Guan et al., *Effect of Suture Properties on Stability of Middle Cerebral Artery Occlusion Evaluated by Synchrotron Radiation Angiography*, *Stroke* **43** (2012) 888.
- [8] G.Q. Zhang et al., *Ring Artifacts Correction Of CT Image Based On Polar Coordinate Transformation*, *Acta Opt. Sin.* **5** (2012) 317.
- [9] H. Q. Liu et al., *Phase Retrieval for Hard X-ray Computed Tomography of Samples with Hybrid Compositions*, *Chinese Opt. Lett.* **10** (2012) 121101.
- [10] Q. Yang et al., *Fast and accurate X-ray fluorescence CT imaging by ordered-subsets expectation maximization algorithm*, *J. Synch. Radiat.* **19** (2012) 210.
- [11] B. Deng et al., *First X-ray fluorescence CT experimental results at SSRF X-ray imaging Beamline*, *Chineses Phys. C* **35** (2011) 402.
- [12] Y.D. Wang et al., *Effects of some factors on X-ray spiral micro-computed tomography at synchrotron radiation*, *Acta Phys. Sin.* **61** (2012) 054205.
- [13] A. Groso et al., *Implementation of a fast method for high resolution phase contrast tomography*, *Opt. Express* **14** (2006) 8103.
- [14] A.V. Bronnikov et al., *The theory of quantitative phase-contrast computed tomography*, *J. Opt. Soc. Am. A* **19** (2002) 472.
- [15] X.Z. Wu et al., *X-ray phase-attenuation duality and phase retrieval*, *Opt. Lett.* **30** (2005) 379.
- [16] T.E. Gureyev et al., *Optical phase retrieval by use of first Born-and Rytov-type approximations*, *Appl. Optics.* **43** (2004) 2418.
- [17] T. Gureyev et al., *Linear algorithms for phase retrieval in the Fresnel region*, *Opt. Commun.* **231** (2004) 53.
- [18] H. Hu, *Multi-slice helical CT: Scan and reconstruction*, *Med. Phys.* **26** (1999) 5.